2022 American Control Conference (ACC)
Atlanta, USA, June 8-10, 2022

Maximizing Harvested Energy in Coulomb Force Parametric Generators

Masoud Roudneshin[1], Kamran Sayrafian[2], Amir G. Aghdam[1]
[1]Department of Electrical Engineering
Concordia University
Montreal, Canada
[2] Information Technology Laboratory
National Institute of Standards & Technology
USA

***Abstract*—Miniaturized wearable or implantable medical sensors are becoming an important application area for kinetic-based micro energy-harvesters. These harvesters can generate power through the natural human body motion. The architecture based on the Coulomb force parametric generator (CFPG) is one of the most viable solutions for these applications. This paper investigates several methods to adaptively estimate the desirable electrostatic force of a CFPG using the acceleration waveform. These methods include an approximate analytical solution based on the mathematical model of the CFPG as well as the least-squares regression and deep learning using artificial neural networks. Simulation results show promising increase in the harvested power using such adaptive strategies.**

I. INTRODUCTION

Energy harvesting (EH) refers to the process of capturing ambient energy from the surrounding environment and converting it into electric energy. A variety of sources such as light, wind, sea waves, heat, and vibrations may be utilized for this conversion. Micro energy-harvesters (MEH), also called micro-generators, typically refer to the class of miniaturized energy harvesting devices that can augment or replace batteries in small low-power electronics. An important application area for micro energy-harvesters includes wearable or implantable medical sensors or actuators [1]–[3]. Since frequent recharge or battery replacement may not be practical (or even feasible for medical implants), integrating micro energy-harvesters with such sensors/actuators could provide a viable solution to extend their operational lifetime.

Several fabrication techniques and architectures for kinetic MEH have been presented and discussed in the literature [4]–[6]. Among such architectures, the Coulomb force parametric generators (CFPG) can harvest the most amount of energy from nonstationary vibration as shown in [7], [8]. Therefore, this architecture is favorable for harvesting kinetic energy from the human body as a non-vibrating source of movements. The energy in a CFPG is produced from the movements of a proof mass between two plates. The proof mass does not vibrate up and down. Instead, a damping force generated by the transducer (i.e., a constant Coulombic electrostatic holding force) tries to keep the proof mass at either of the plates. The proof mass is held against one plate until the external acceleration exceeds the holding force threshold. Power is only generated when the proof mass makes a full flight from one plate to the other. Utilizing electrostatic force rather than electromagnetic or piezoelectric forces is another advantage of the CFPG architecture. Any of these forces can be used to generate electrical power by converting mechanical energy into an electrical form. However, the electrostatic force becomes more significant on the micro-scale, and therefore, is more suitable for electrical power generation [8]. As a result, the transduction method in CFPG architecture allows for the miniaturization of the harvester's size; a highly desirable feature for wearable and implant applications.

The potential impact of the electrostatic force on the generated power has been investigated in [10]–[12]. This damping force is typically set to a constant value. However, by adaptively changing its value for various human body motions, it is expected to increase the amount of harvested energy for wearable and implant sensors. The adjustment of this electrostatic force within the microgenerator hardware can be done by tuning the electric field between the CFPG's capacitive electrodes, i.e., plates [12].

The average output power of a CFPG for various constant values of the electrostatic force and different daily human activities such as running and walking is investigated in [10]. A statistical analysis of the human body acceleration is used in [11] to find an upper bound on the harvested power using a CFPG. The authors in [12] propose a mathematical model of the CFPG to more accurately study the instantaneous power generated by the device. Furthermore, they formulate an optimization problem for adaptive adjustment of the electrostatic force based on the input acceleration signal. The main concept behind this optimization problem is the identification of a mapping from the acceleration waveform to the optimal holding/electrostatic force. Although implementation of this mapping in real-time and without any time delay might not be practical, the temporal correlation in the acceleration waveform generated by the human motion

978-1-6654-5196-3/$31.00 ©2022 AACC

translates to an almost constant value of the optimal holding force for sufficiently small time interval. This could allow the practical implementation of a mapping that can estimate the near-optimal value of the electrostatic force based on the experienced acceleration in the immediate past. The preliminary results of a machine learning-based approach to solving this optimization problem are presented in [14], [15]; however, a more comprehensive analysis of the solutions with performance evaluation for various human activities is still needed.

In this paper, we present various techniques to adaptively optimize the electrostatic force in a CFPG and evaluate the resulting gain in the output power. The proposed techniques include an approximate analytical approach, deep learning (DL) and least square methods. The performance of these approaches is evaluated for sample measured acceleration data representing various human activities. To the authors' best knowledge, output power maximization of CFPG through adaptive electrostatic force has not been comprehensively studied before.

The rest of this paper is organized as follows. Section II presents the mathematical model of a CFPG and describes the adaptive power maximization problem. Acceleration data measurement and the corresponding experiments are provided in Section III. In Section IV, different methodologies for adaptive optimization of the electrostatic force with simulation results are presented. Finally, conclusions and some future research directions are outlined in Section V.

II. Problem Definition

In this section, the mathematical model of a CFPG is given and the adaptive optimization problem is formulated.

A. Mathematical Model

The generic model of the core component in a CFPG architecture is shown in Fig. 1. As observed from this figure, the proof mass is able to move between the upper and lower plates. Depending on its movement direction, the maximum travel distance to reach either plate is denoted by $\pm Z_l$. Energy is converted when work is done by the proof mass to complete a full journey from one plate to the other against the transducer's damping force which opposes the relative motion of the proof mass [7], [8]. The direction of the damping force is reversed when the proof mass completes its journey. Kinetic energy is harvested from the human body motion every time this complete journey of the proof mass takes place.

Let $y(t)$ denote the device motion with respect to the inertial frame and $z(t)$ be the relative motion of the mass with respect to the device's frame. As presented in [12], the following nonlinear differential equation effectively models the dynamic of a CFPG:

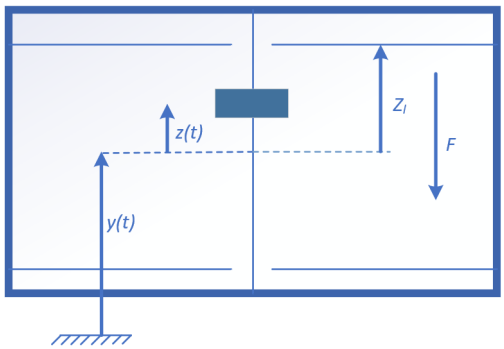

Fig. 1. The generic model of the core component in a CFPG

$$m\ddot{y}(t) = -m\ddot{z}(t) + F \times \text{Relay}(z(t)), \tag{1}$$

where m denotes the mass of the proof mass, $\ddot{z}(t)$ denotes the relative acceleration of the proof mass with respect to the CFPG frame, $\ddot{y}(t)$ is the acceleration of the inertial frame, and F denotes the electrostatic (also referred to as holding) force. The function Relay(.) acts as a hysteresis loop and is plotted in Fig. 2.

The mechanical power generated by the proof mass is given by:

$$P(t) = F \times \dot{z}(t), \tag{2}$$

where $\dot{z}(t)$ is the relative velocity of the proof mass with respect to the frame. It is important to note that the power remains positive as long as the direction of $\dot{z}(t)$ is opposite to the electrostatic force. If the proof mass reverses course before reaching the other plate and returns to the starting plate, the sign of the generated power in (2) will turn negative. This will nullify the positive power generated up to that point, leading to a zero-average value of the generated power.

Aside from the input acceleration, other factors that can impact the amount of harvested power are the size of the proof mass, the distance between the two plates that the proof mass can traverse and, in particular, the value of the electrostatic force.

B. Optimization of the Output Power

Assuming that the electrostatic force can be adjusted every Δ_i seconds, the objective is to estimate its optimal value at each time interval to maximize the average harvested power as follows:

$$\underset{F_i^{\Delta_i}, \Delta_i}{\text{argmax}} \left[\frac{1}{\sum_{i=1}^{N} \Delta_i} \times \sum_{i=1}^{N} \int_{t_i - \Delta_i}^{t_i} P(t)dt \right], \tag{3}$$

where Δ_i denotes the optimal decision interval i, N is the number of decision intervals, $F_i^{\Delta_i}$ is the optimal constant electrostatic force in the ith interval and $P(t)$

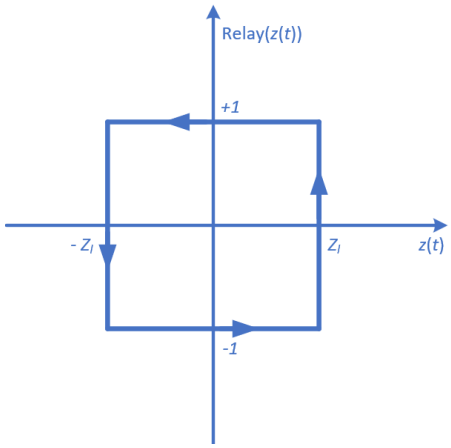

Fig. 2. Relay function

is the instantaneous output power. For simplicity, let the length of the decision interval be fixed and denoted by Δ. Equation (3) can then be written as:

$$\underset{F_i{}^{\Delta}}{\operatorname{argmax}} \left[\frac{1}{N\Delta} \times \sum_{i=1}^{N} \int_{t_0+(i-1)\Delta}^{t_0+i\Delta} P(t)dt \right]. \quad (4)$$

The optimal electrostatic force is a function of both the decision interval length Δ and the acceleration waveform during the ith interval, i.e., $[t_0 + (i-1)\Delta, t_0 + i\Delta]$. This can be described as the mapping function ϕ that estimates $F_i{}^{\Delta}$ as stated in the equation below:

$$\phi : [\mathbf{x}_1(i), ..., \mathbf{x}_M(i)] \rightarrow F_i{}^{\Delta} \quad (5)$$

where $\mathbf{x}_k(i)$ denotes the kth sample from the acceleration waveform k = 1, 2, ..., M during the ith time interval. It should be noted that using (4), the estimated optimal electrostatic force $F_i{}^{\Delta}$, hereafter referred to as F_i, at time $t_0 + i\Delta$ is obtained based on the input acceleration samples during the immediate past time interval. As mentioned before, this is possible due to the inherent temporal correlation in the human body motion. Several techniques for this estimator are presented in Section IV.

III. Acceleration Data Acquisition

To measure acceleration from the human body motions, we used the X16-mini triaxial accelerometer developed by Gulf Coast Data Concepts, LLC[1]. The dimensions of this device are 51×25×13mm^3. It is small enough to be comfortably placed at various locations on the body to collect data. Body acceleration data is measured along three orthogonal axes. The measurement

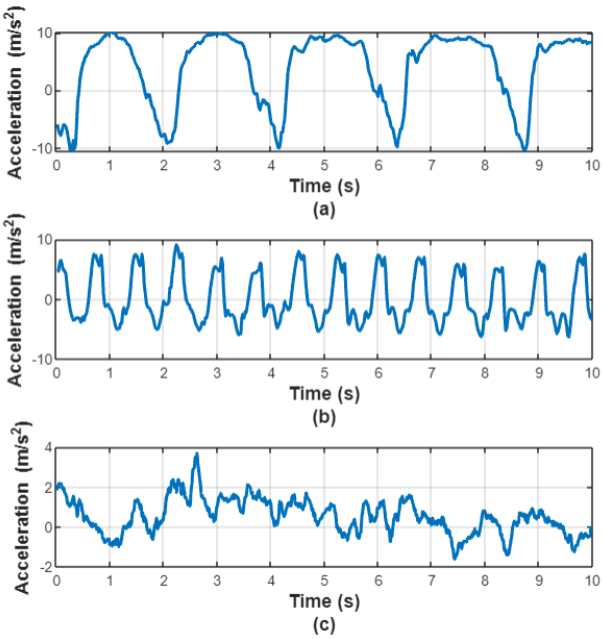

Fig. 3. Acceleration waveform samples for: (a) sit-ups, (b) jogging, (c) random movements of hand and shoulder (Accelerometer placed on the left wrist with moderate level of activity)

samples are time-stamped and stored in the device for later retrieval. The sampling rate of the device can be selected to be 12, 25, 50, 100, 200, 400, or 800Hz. Data are collected from various daily physical activities such as walking, jogging, sit-ups, roping, weight exercises and general random movements of hand and shoulder[2]. Data from each activity are collected for 5 minutes with the accelerometer attached on the volunteers' wrist, biceps, leg and chest. To account for changes in the frequency and amplitude of the acceleration waveform, we conducted data collection for three levels of slow, moderate, and intense activities. Fig. 3 shows several sample acceleration waveforms obtained from our experiments. The spectral content of these waveforms can be derived using the Fourier Transform of the time domain data; the results are shown in Fig. 4. As observed, the spectral content of these activities is mostly below 5Hz. However, a maximum frequency of 10Hz was observed in our measurements for rapid hand movements. The frequency spectrum of the measured waveforms may include a dc component (i.e., bias) which is due to the impact of gravity on the accelerometer. This component has been eliminated from the dataset by proper filtering.

[1]Commercial products mentioned in this paper are merely intended to foster research and understanding. Such identification does not imply recommendation or endorsement by the National Institute of Standards and Technology.

[2]The experiments were conducted according to the research ethics regulations under the approval number 30013664 at Concordia University and ITL-2021-0273 at NIST.

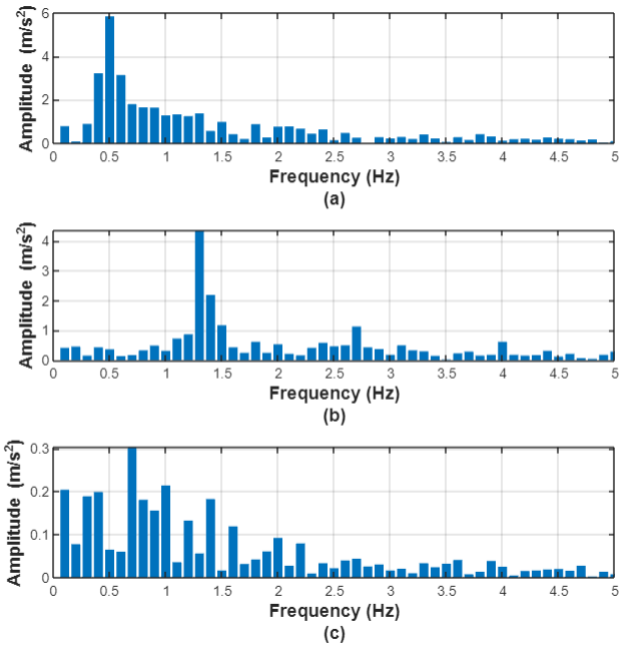

Fig. 4. Frequency spectrum of the acceleration waveform samples shown in Fig. 3: (a) sit-ups, (b) jogging, (c) random movements of hand and shoulder

IV. Main Results

In this section, different computational methods for estimating the near-optimal electrostatic force are proposed and their performance are evaluated using the dataset discussed in the previous section.

A. Approximate Analytical Approach

Let the input acceleration signal be sampled at T-second intervals, and discretize (1) as:

$$m\ddot{y}[n] = -m\ddot{z}[n] + F[n] \times \text{Relay}(z[n]) \qquad (6)$$

where $y[n] := y(nT)$ (all other discrete-time functions and variables are defined similarly). Let the second derivative of z in the above equation be replaced with its numerical approximation over one sampling interval, which results in:

$$\dot{z}[n] = -T\ddot{y}[n] + \dot{z}[n-1] + \frac{TF[n]}{m} \times \text{Relay}(z[n]) \quad (7)$$

Multiplying the above equation by $F[n]$ yields:

$$\dot{z}[n]F[n] = (-T\ddot{y}[n] + \dot{z}[n-1])F[n] + \left(\frac{T}{m} \times \text{Relay}(z[n])\right)F^2[n] \qquad (8)$$

The above equation, according to (2), provides the power generated at each discrete time instant n. Equation (8) indicates that $P[n]$ is a parabolic function of the electrostatic force $F[n]$. Let the proof mass be initially attached to the lower plate and stationary. Equation (8) can then be rewritten as:

$$P[n] = (-T\ddot{y}[n])F[n] + \left(\frac{T}{m}\right)F^2[n] \qquad (9)$$

Taking the derivative of power with respect to the electrostatic force, using the discrete-time approximation, and setting it to zero yields:

$$F_{aa}[n] = \frac{m\ddot{y}[n]}{2} \qquad (10)$$

Given the simplifying assumptions stated above, equation (10) provides the estimate of the optimal electrostatic force over one sampling period. Fig. 5 shows the performance of this method (i.e., adaptively adjusting the holding force). A sampling rate of 100Hz has been used to obtain this result. The curves in Fig. 5 demonstrate the output harvested energy for 100s of mixed activity data obtained experimentally. The harvested energy is illustrated for three cases. An adaptive electrostatic force is applied according to equation (10) in the first case. In the second one, a constant electrostatic force equal to 3mN is applied; the constant force is denoted by F_{constant}. Finally, in the third case, the optimal force F_{opt} obtained through exhaustive search with a decision interval of Δ = 2s is used as the best achievable performance. Using this adaptive approach, roughly 60% of the maximum output power which would have been generated under the optimal scheme can be obtained.

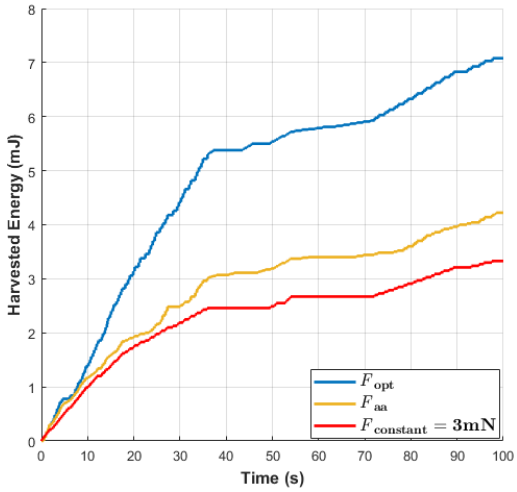

Fig. 5. Harvested energy for the proposed analytical method compared to that for the optimal and a constant holding force

B. Least-Squares Approach

Consider estimating the holding force by a linear mapping based on the acceleration data samples during

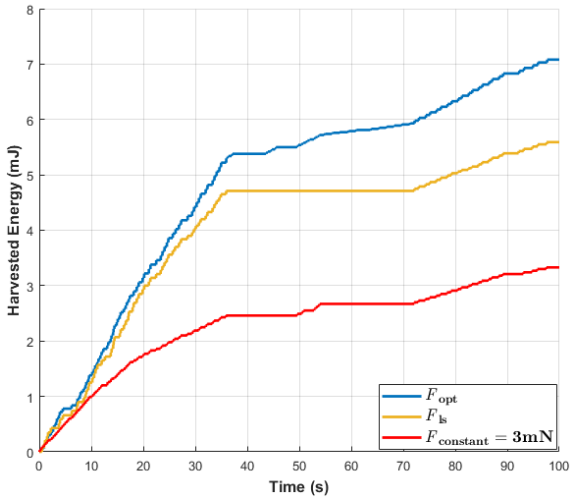

Fig. 6. Harvested energy for the proposed least-squares method compared to that for the optimal and a constant holding force

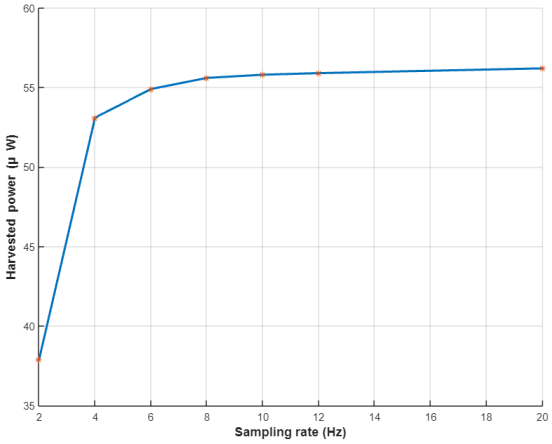

Fig. 7. Harvested power versus sampling rate for the least-squares approach

the ith interval as follows:

$$\theta_1 \ddot{y}_i[1] + \cdots + \theta_M \ddot{y}_i[M] = F_{ls}(i) \tag{11}$$

where $\ddot{y}_i[k]$ is the kth measured sample acceleration and $F_{ls}(i)$ is the estimated holding force k = 1, ..., M both at the ith decision interval. To find proper coefficients (θ_i) to estimate the electrostatic force $F_{ls}(i)$, we consider the following minimization problem:

$$\underset{\boldsymbol{\theta_1},\ldots,\boldsymbol{\theta_M}}{\text{minimize}} \quad ||\mathbf{F}_{\text{opt}} - \ddot{\mathbf{Y}}\boldsymbol{\Theta}||, \tag{12}$$

where

$$\mathbf{F}_{\text{opt}} = [F_{\text{opt}}(1), ..., F_{\text{opt}}(N)],$$

and

$$\boldsymbol{\Theta} = [\theta_1, ..., \theta_M]^\intercal,$$

and $\ddot{\mathbf{Y}}$ is a $M \times N$ matrix of M acceleration measurements for N decision intervals. We seek to minimize the norm of the discrepancy between the estimates and the optimal values. In fact, equation (12) is an L_2-norm approximation problem. Note that in practice, $\ddot{\mathbf{Y}}$ is a tall matrix that can be constructed using the measurement dataset discussed in the previous section. The solution of the least-squares problem in this case is given by:

$$\boldsymbol{\Theta} = (\ddot{\mathbf{Y}}^\intercal \ddot{\mathbf{Y}})^{-1} \ddot{\mathbf{Y}}^\intercal \mathbf{F}_{\text{opt}} \tag{13}$$

Remark 1: The choice of M in (11) is essential in the numerical computation of the estimated parameters. If the input samples in the least-squares problem are not selected sufficiently distinct from each other, $\ddot{\mathbf{Y}}^\intercal \ddot{\mathbf{Y}}$ in (13) will be close to a singular matrix, causing numerical problems.

Fig. 6 demonstrates the performance of this methodology with $\Delta = 2$s in comparison with that resulted from the optimal and constant values for the electrostatic force. A sampling rate of 10Hz (i.e., M = 20) has been used in this figure. Compared to the optimal scheme, nearly 78% of the maximum output power can be achieved when the least-squares approach is used to adapt the holding force.

The computational complexity of this approach is directly related to the number of acceleration samples (i.e. M) used to estimate the electrostatic force as shown in equation (13). The number of samples depends on the sampling frequency of the acceleration signal. A lower M, or equivalently a lower sampling rate, could deteriorate accuracy; and therefore, reduce the harvested power. However, the resultant computational complexity would be lower as well. Fig. 7 shows the variation of the harvested power when the sampling rate increases from 2Hz to 20Hz. An increase of roughly 10% in the output power is observed when the sampling rate increases from 2Hz to 10Hz. However, no noticeable change in the harvested power is observed beyond 10Hz. This result is consistent with the fact that no frequency content above 10Hz was observed in our measurement dataset. When the sampling rate is 10Hz, the harvested energy is within 78% of the power that could have been obtained following the optimal scheme.

C. Deep Learning Approach

Deep Learning (DL) is a type of machine learning based on artificial neural networks (ANN) in which multiple layers of processing are used to establish a relationship between sensory stimuli and the output. In other words, DL can be used to uncover the underlying mapping function from the input data to a desired output. Here, we investigate how a DL architecture based on multi-layer artificial neural network can be used to estimate the optimal electrostatic force based on

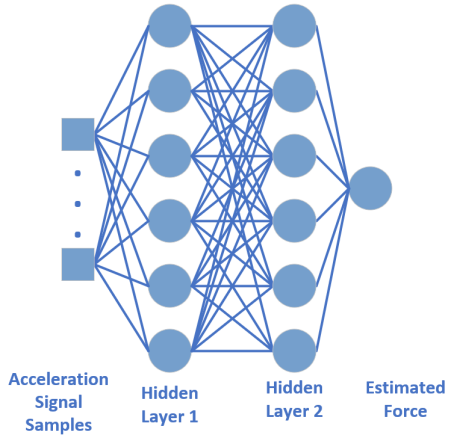

Fig. 8. Generic model of a deep neural network

input acceleration data. A four-layer neural network is proposed in Fig. 8 to represent the mapping from the input to the desired holding force. Each node in this architecture, except the nodes on the first hidden layer, applies a nonlinear activation function to the weighted sum of its inputs, and then passes the output to the next layer. Tangent hyperbolic has been chosen as the activation function of our proposed DL approach. The inputs to the ANN are samples of the acceleration waveform in time. The ANN output is the estimated electrostatic force that will be used for the next time interval.

To find a proper mapping from the input to the output, the set of weights $\mathbf{w} := [w_{ji}]$ (associated with the ith neuron at the jth layer) has to be determined through the training process. The measurement database described in Section III can be used to perform this training. To this end, the following cost function is defined to measure the performance of the neural network:

$$\mathcal{L}(\mathbf{w}) = \frac{1}{2K}\sum_{i=1}^{K}|F_i - F_{DL}(i)|^2, \tag{14}$$

where K is the number of training examples, F_{DL} denotes the estimated holding force from the ANN, and F_i denotes the desired value of the electrostatic force obtained through exhaustive search. Proper values for the weights and biases are derived through a gradient descent algorithm in the following general form:

$$w_{ji}^{k} = w_{ji}^{k-1} - \alpha\frac{\partial\mathcal{L}}{\partial w_{ji}^{k-1}}$$

where α is a learning rate between 0 and 1 (often adjusted by trial and error).

To implement the 4-layer ANN, Keras library in Python is utilized. Using the same decision interval of Δ = 2s and a sampling rate of 10Hz, the results in Fig. 9 are obtained which demonstrate the performance of this methodology in comparison with the optimal and constant electrostatic force. Measurement samples of the acceleration signal in time are used for training the ANN. The estimated holding force based on this approach is denoted by $F_{DL_{time}}$. With the sampling rate of 10Hz, 20 acceleration samples in the time domain at each decision interval were used at the input layer to train the ANN. As observed in Fig. 9, this method performs significantly better than the constant electrostatic force (F_{constant}= 3mN), nearing 85% of the maximum power harvested under the optimal scheme.

The complexity of the DL approach depends on several factors such as the size of the input layer, number of nodes per layer in the ANN architecture and the nonlinear activation function used. The impact of the input layer size can be studied by changing the sampling rate of the acceleration signal in the time domain or using different number of frequency components to train the ANN. In the time domain approach, a lower sampling rate would result in a smaller number of samples during the decision interval and therefore, a smaller input layer. This would also impact the size of the hidden layers, hence, reducing the required computational complexity of the ANN. Fig. 10 depicts the variation of the harvested power versus sampling rate. As shown in this figure, reducing the sampling rate from 10Hz to 2Hz reduces the harvested power by around 7%. However, the corresponding computational complexity reduces significantly as well. Also, as expected, there is no improvement in the output power when the sampling rate increases beyond 10Hz. This is again due to the fact that no frequency content above 10Hz was observed in the dataset collected in our experiments.

V. Conclusions

The output power maximization of a Coulomb force parametric generator through adaptation of the electrostatic force based on the acceleration waveform was studied. Several techniques were proposed for this adaptation, including (i) an approximate analytical solution derived from the mathematical model of the CFPG, (ii) an artificial neural network trained with time-domain data obtained from physical experiments, and (iii) the least-squares regression using the collected data. Although the ANN resulted in the highest increase in the harvested power, it also involves the highest computational complexity for implementation. This complexity could reduce the overall gain in the output power of the micro-generator. Note that estimating the required computational power for each adaptation method is essential to determine the net gain in the harvested energy. Approximation of the input acceleration waveform with few frequency components and implementation of the

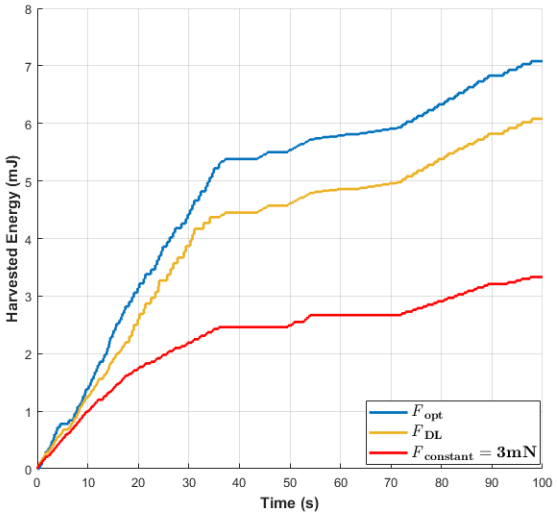

Fig. 9. Harvested energy for the proposed deep learning method compared to that for the optimal and a constant holding force

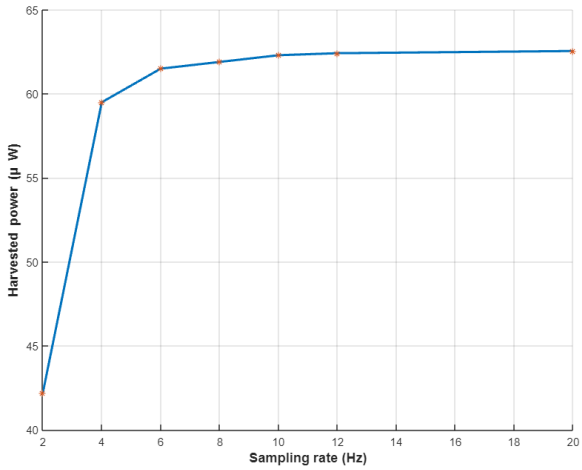

Fig. 10. Harvested power versus sampling rate for $F_{DL_{time}}$ approach

deep learning approach in the frequency domain is a possible future research direction. In addition, studying the impact of the length of the decision interval and discretization of the holding force on the harvested power is another topic of interest for further research.

ACKNOWLEDGEMENT

This work was supported by the National Institute of Standards and Technology (NIST) under grant number 60NANB20D163.

REFERENCES

[1] H. C. Koydemir and A. Ozcan, "Wearable and Implantable Sensors for Biomedical Applications," *Annual Review of Analytical Chemistry*, vol. 11, pp. 127–146, 2018.

[2] Y. Khan, A. E. Ostfeld, C. M. Lochner, A. Pierre, and A. C. Arias, "Monitoring of Vital Signs with Flexible and Wearable Medical Devices," *Advanced Materials*, vol. 28, no. 22, pp. 4373–4395, 2016.

[3] D. Briand, E. M. Yeatman, S. Roundy, "Introduction to Micro Energy Harvesting," *Micro Energy Harvesting*. 2015 May 8:1-5.

[4] K. Li, Q. He, J. Wang, Z. Zhou, X. Li, "Wearable Energy Harvesters Generating Rlectricity from Low-frequency Human Limb Movement," *Microsystems & Nanoengineering*. 2018 Sep. 10;4(1):1-3.

[5] C. Cepnik, R. Lausecker, U. Wallrabe, "Review on Electrodynamic Energy Harvesters—A Classification Approach," *Micromachines*. 2013 Jun. ;4(2):168-196.

[6] A. Cadei, A. Dionisi, E. Sardini, M. Serpelloni, "Kinetic and Thermal Energy Harvesters for Implantable Medical Devices and Biomedical Autonomous Sensors," *Measurement Science and Technology*. 2013 Nov. 13;25(1):012003.

[7] P. D. Mitcheson, "Analysis and Optimisation of Energy-Harvesting Micro-Generator Systems," *Ph.D. Dissertation,* Imperial College London, 2005.

[8] P. D. Mitcheson, T. Sterken, C. He, E. M. Kiziroglou, E. M. Yeatman, and R. Puers, "Electrostatic Microgenerators," *Measurement and Control*, vol. 41, no. 4, pp. 114–119, 2008.

[9] F. K. Shaikh and S. Zeadally, "Energy Harvesting in Wireless Sensor Networks: A Comprehensive Review," *Renewable and Sustainable Energy Reviews*, vol. 55, pp. 1041–1054, 2016.

[10] D. Budić, D. Šimunić, and K. Sayrafian, "Kinetic-Based Micro Energy-Harvesting for Wearable Sensors," in *Proceedings of the 6th IEEE International Conference on Cognitive Infocommunications (CogInfoCom)*, 2015.

[11] N. Yarkony, K. Sayrafian, and A. Possolo, "Energy Harvesting from the Human Leg Motion," in *Proceedings of the 8th International Conference on Pervasive Computing Technologies for Healthcare*, pp. 88–92, 2014.

[12] M. Dadfarnia, K. Sayrafian, P. D. Mitcheson, and J. S. Baras, "Maximizing Output Power of a CFPG Micro Energy-Harvester for Wearable Medical Sensors," in *Proceedings of the 4th International Conference on Wireless Mobile Communication and Healthcare-Transforming Healthcare Through Innovations in Mobile and Wireless Technologies (MOBIHEALTH)*, 2014.

[13] T. Von Buren, P. D. Mitcheson, T. C. Green, E. M. Yeatman, A. S. Holmes, G. Troster, "Optimization of Inertial Micropower Generators for Human Walking Motion," *IEEE Sensors journal*. 2006 Jan. 16;6(1):28-38.

[14] M. Roudneshin, K. Sayrafian, and A. G. Aghdam, "A Machine Learning Approach to the Estimation of Near-Optimal Electrostatic Force in Micro Energy-Harvesters," in *Proceedings of the IEEE International Conference on Wireless for Space and Extreme Environments (WiSEE)*, 2019.

[15] M. Roudneshin, K. Sayrafian, and A. G. Aghdam, "Adaptive Estimation of Near-Optimal Electrostatic Force in Micro Energy-Harvesters," in *Proceedings of the IEEE International Conference on Control Technology and Applications (CCTA)*, 2020.